A New Two-Degree-of-Freedom Space Heating Model for Demand Response

Anita Sant'Anna[1] and Robert Bass[2]
[1]*Embedded and Intelligent Systems Research Group, Halmstad University, Halmstad, Sweden*
[2]*Department of Electrical & Computer Engineering, Portland State University, Portland, OR, U.S.A.*

Keywords: Space Heating, Demand Response, Thermal Comfort, Thermodynamic Model, Simulation.

Abstract: In today's fast changing electric utilities sector demand response (DR) programs are a relatively inexpensive means of reducing peak demand and providing ancillary services. Advancements in embedded systems and communication technologies are paving the way for more complex DR programs based on transactive control. Such complex systems highlight the importance of modeling and simulation tools for studying and evaluating the effects of different control strategies for DR. Considerable efforts have been directed at modeling thermostatically controlled appliances. These models however operate with only one degree of freedom, typically, the thermal mass temperature. This paper proposes a two-degree-of-freedom residential space heating system composed of a thermal storage unit and forced convection system. Simulation results demonstrate that such system is better suited for maintaining thermal comfort and allows greater flexibility for DR programs. The performance of several control strategies are evaluated, as well as the effects of model and weather parameters on thermal comfort and power consumption.

1 INTRODUCTION

The electric utilities sector currently faces a number of challenges: how to manage electricity prices in an unregulated market (Spees and Lave, 2007), how to cope with more distributed and intermittent generation such as wind power (Kondoh et al., 2011), as well as how to cope with ever increasing peak demands (Ericson, 2009). Demand response (DR) programs are an effective means for alleviating such issues. When consumers can respond in real time to high electricity prices, they naturally tend to reduce peak-time usage, and consequently help equalize demand and prices (Spees and Lave, 2007). In addition, DR programs provide a more flexible and efficient option for fast-response ancillary services (Kondoh et al., 2011).

Albadi *et al.* concisely summarized a hierarchy of current incentive- and price-based utility DR programs (Albadi and El-Saadany, 2007). Incentive-based residential programs often take the form of direct control, wherein a utility can directly apply an on/off duty cycle to customer appliances in order to adjust aggregate customer demand. Often, such programs are used for load shedding during high-demand periods. In return for taking part in such programs customers are rewarded with an incentive, such as a discount on their electricity bill. Incentive-based DR has been considered in works such as (Mohsenian-Rad et al., 2010).

Price-based programs, on the other hand, persuade customers to change their electricity consumption behavior by adjusting prices throughout day. Price adjustments occur either in response to current demand or are based on a predetermined time-of-use schedule. Participating customers may therefore avoid high electricity prices by modifying their behavior, such as reducing consumption during peak-periods. Price-based DR has been considered in works such as (Fuller et al., 2011).

Current developments in embedded system technologies and communications make it possible to implement home energy management (HEM) systems that not only react to but also interact with the grid through mechanisms like transactive control (Schneider et al., 2011), (Chassin et al., 2008). In the future, distributed HEM systems will be an integral part of DR programs (Pipattanasomporn et al., 2012). Modeling and simulation tools are essential in understanding and evaluating the effects of different DR control strategies prior to large scale deployment. In this context, it is important to create residential load models

Sant'Anna A. and Bass R..
A New Two-Degree-of-Freedom Space Heating Model for Demand Response.
DOI: 10.5220/0004734600050013
In *Proceedings of the 3rd International Conference on Smart Grids and Green IT Systems* (SMARTGREENS-2014), pages 5-13
ISBN: 978-989-758-025-3

that simulate the physical behavior of appliances participating in DR programs (Shao et al., 2013).

Thermostatically controlled appliances (TCA), such as water heaters and HVAC systems, are of particular interests because they can store thermal energy. Intelligent control strategies can make use of this storage capacity in order to avoid operating during peak periods with little inconvenience to the customer. A 2001 survey by the Office of Energy Markets and End Use (RECS, 2001) reported that 9.1% of household electricity consumption was due to water heaters. Another considerable amount, 10.1%, was due to space heating. Several pilot programs have been conducted that employ hot water heaters as the DR appliance, particularly in the U.S. states of Washington and Oregon (Kondoh et al., 2011), (Chassin et al., 2008), (Diao et al., 2012), as well as in Norway (Saele and Grande, 2011).

Considerable efforts have been directed to modeling thermostatically controlled loads. The thermodynamic behaviors of electric water heaters and HVAC system are normally described by differential equations (Lu, 2012), (Du and Lu, 2011), (Molina-Garcia et al., 2011). Often, the system presents two behaviors: on or off. When the appliance is on, the temperature of the thermal mass increases following a negative exponential curve ($c - e^{-\tau}$); when then appliance is off, the temperature of the thermal mass decreases exponentially ($c + e^{-\tau}$) (Lu et al., 2005). The time constant τ relates to the thermal capacitance of the thermal mass.

However, the above mentioned models present only one degree of freedom (DoF) for control, typically, the desired indoor temperature or the minimum and maximum acceptable temperatures for the thermal mass (Pipattanasomporn et al., 2012). This paper introduces a two-DoF space heating model composed of a heat pump, a thermal storage unit (hot water tank) and a forced convection system. The heat pump transfers thermal energy to the thermal storage and heats up the water. The hot water is circulated through coiled pipes, transferring heat to it surrounding air, which is in turn circulated through the house by the forced convection system. Such systems contain, in effect, two thermal masses: the thermal storage unit and the thermal mass of the house (air and structures). These systems are not new, they are common in Canada and in Nordic countries, however, they have not yet been considered in DR studies.

This paper demonstrates that two-DoF systems are better adapted for maintaining thermal comfort and allow greater flexibility for DR programs. The DR performance of the proposed system is compared to a traditional one-DoF system through simulations. The systems are evaluated with respect to their ability to maintain indoor temperature within a comfortable range (Peeters et al., 2009). Simple control strategies are proposed for the forced convection system coupled to on-off, and multistage compressors. Simulation results show the importance of considering two-DoF models for DR.

The contributions of this paper may be summarized as follows.

- The description of a two-DoF heating system model composed of an insulated thermal storage unit and a forced convection system (FCS);
- The comparison and evaluation of two-DoF and one-DoF systems for price-based DR;
- The evaluation of different control strategies for two-DoF systems, and their effect on thermal comfort for on/off, and multistage compressors as well as three different weather profiles;

The remainder of the paper is organized as follows. Thermodynamic model and control strategies are described in Section 2. Model and simulation parameters used for the study are explained in Section 3. Simulation results are presented in Section 4 and discussed in Section 5. Finally, Section 6 concludes this paper.

2 MODELS

2.1 Thermodynamic Model

The proposed system consists of:

- A rectangular volume with insulated walls representing the house.
- An insulated thermal energy storage unit (hot water tank).
- A heat pump directly coupled to the thermal mass.
- A forced convection system (FCS) that transfers heat from the thermal mass to the house.

This thermodynamic model can be represented as a thermal circuit, as shown in Figure 1. The equivalent mathematical model is shown in Equation (2), where T_H is the indoor temperature; T_{TM} is the thermal mass temperature; and T_O is the ambient outdoor temperature. The mass of the water in the storage tank is m_{TM} and its specific heat is C_{TM}. The heat storage capacity of the house is represented by the capacitance of value $C_H m_H$, which includes the heat capacity of the air contained in the house as well as it's structure and materials. The heat conductivity between the thermal mass and the house is represented

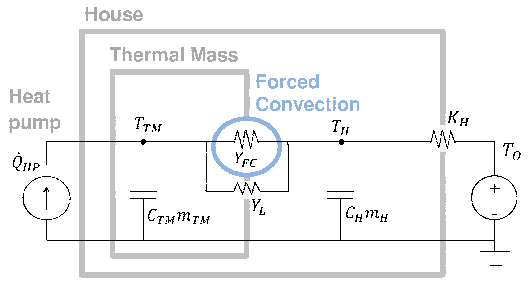

Figure 1: Thermal circuit representation of the thermodynamic model. T_H is the indoor temperature; T_{TM} is the thermal mass temperature; and T_O is the ambient outdoor temperature. The mass of the water in the storage tank is m_{TM} and its specific heat is C_{TM}. The heat storage capacity of the house is represented by the capacitance of value C_Hm_H, which includes the heat capacity of the air contained in the house as well as it's structure and materials. The heat conductivity between the thermal mass and the house is represented by Y_{TM-H}, which depends on the heat transfer coefficient created by the FCS, Y_{FC}, and the thermal mass heat loss, Y_L, according to equation 1. The conductivity of the house insulation is represented by K_H; and $\dot{Q}_{HP}$ is the heat pump's thermal power output.

by Y_{TM-H}, which depends on the heat transfer coefficient created by the FCS, Y_{FC}, and the thermal mass heat loss, Y_L, according to Equation 1. The conductivity of the house insulation is represented by K_H; and $\dot{Q}_{HP}$ is the heat pump's thermal power output.

It is worth noting that, if the conductivity between the thermal mass and the house Y_{TM-H} is kept constant, this model is qualitatively no different from previously proposed models (Lu, 2012), (Du and Lu, 2011), (Molina-Garcia et al., 2011). However, by considering an insulated thermal mass coupled with a FCS, the indoor temperature is introduced as a new degree of freedom, in addition to the temperature of the thermal mass.

$$Y_{TM-H} = Y_{FC} + Y_L \tag{1}$$

$$\dot{T}_H = \frac{K_H(T_O - T_H) - Y_{TM\text{-}H}(T_H - T_{TM})}{m_H C_H} \tag{2a}$$

$$\dot{T}_{TM} = \frac{\dot{Q}_{HP} - Y_{TM\text{-}H}(T_{TM} - T_H)}{m_{TM} C_{TM}} \tag{2b}$$

2.2 Forced Convection System Model and Control

Consider a FCS that can operate in two fan speed modes, low and high. The two modes are modeled as different heat transfer coefficients between the thermal mass and the house, $Y_{FC\text{-}low}$ and $Y_{FC\text{-}high}$ respectively. The output of the FCS is controlled by a set of if-then rules based on the ambient indoor temperature, T_H, as shown in Equation (3). The total heat transfer between the thermal mass and the house is computed from Equation 1.

$$Y_{FC} = \begin{cases} 0 & \text{if } T_H > T_{H\text{-}goal} \\ Y_{FC\text{-}low} & \text{if } T_{H\text{-}goal}-1 < T_H \leq T_{H\text{-}goal} \\ Y_{FC\text{-}high} & \text{if } T_H \leq T_{H\text{-}goal}-1 \end{cases} \tag{3}$$

2.3 Heat Pump Model and Control

We consider a multistage heat pump capable of three modes of operation: low, medium and high. The thermal power supplied by each operation mode will be referred to as $\dot{Q}_{HP\text{-}low}$, $\dot{Q}_{HP\text{-}med}$ and $\dot{Q}_{HP\text{-}high}$ respectively.

In order to avoid modeling a short-cycled compressor, we assume that the heat pump may not be switched on and off in less than 5 minutes.

Operation is also affected by the demand response program, which requires the pump to switch off during peak periods, represented by the time-of-use rate $TUR_{on\text{-}peak}$.

Four different control scenarios are considered:

- **Case I**: A traditional one-DoF system where the indoor temperature is directly coupled to the thermal storage temperature, and consequently, to the heat pump output. The heat transfer coefficient between the thermal mass and house is constant, $Y_{TM\text{-}H} = Y_{FC\text{-}low} + Y_L$. This scenario considers a heat pump with only on/off operation. The heat pump output is controlled based on the indoor temperature as shown in Equation (4).

$$\dot{Q}_{HP} = \begin{cases} 0 & \text{if } T_H > T_{H\text{-}goal} \text{ or } TUR_{on\text{-}peak} \\ \dot{Q}_{HP\text{-}high} & \text{if } T_H \leq T_{H\text{-}goal}-1 \end{cases} \tag{4}$$

- **Case II**: A simple two-DoF system where the indoor temperature and the thermal storage temperature are controlled separately. The FCS is responsible for regulating the indoor temperature and the heat pump is responsible for regulating the thermal mass temperature. The heat pump is either on or off, and its output is controlled based on the thermal mass temperature as shown in Equation (5). The FCS operates as shown in Equation (3).

$$\dot{Q}_{HP} = \begin{cases} 0 & \text{if } T_{TM} > T_{TM\text{-}goal} \text{ or } TUR_{on\text{-}peak} \\ \dot{Q}_{HP\text{-}high} & \text{if } T_{TM} \leq T_{TM\text{-}goal} - 2 \end{cases} \quad (5)$$

- **Case III**: This scenario considers the previous two-DoF system but with a multistage heat pump that can operate in three different modes: low, medium or high. The operation mode selection is done through a collection of if-then rules based on the thermal mass temperature as shown in Equation (6). The FCS operates as shown in Equation (3).

$$\dot{Q}_{HP} = \begin{cases} 0 & \text{if } T_{TM} > T_{TM\text{-}goal} \text{ or } TUR_{on\text{-}peak} \\ \dot{Q}_{HP\text{-}low} & \text{if } T_{TM\text{-}goal} - 1 < T_{TM} \leq T_{TM\text{-}goal} \\ \dot{Q}_{HP\text{-}med} & \text{if } T_{TM\text{-}goal} - 3 < T_{TM} \leq T_{TM\text{-}goal} - 1 \\ \dot{Q}_{HP\text{-}high} & \text{if } T_{TM} \leq T_{TM\text{-}goal} - 3 \end{cases} \quad (6)$$

- **Case IV**: This final scenario considers the previous two-DoF system with a multi-stage heat pump. The heat pump output selection, however, is done with the help of a PD controller as shown in Equation (7). The FCS operates as shown in Equation (3).

$$\dot{Q}_{ctrl} = k_P(T_{TM\text{-}goal} - T_{TM}) + k_D \dot{T}_{TM} \quad (7a)$$

$$\dot{Q}_{HP} = \begin{cases} 0 & \text{if } \dot{Q}_{ctrl} \leq \dot{Q}_{HP\text{-}low} \text{ or } TUR_{on\text{-}peak} \\ \dot{Q}_{HP\text{-}low} & \text{if } \dot{Q}_{HP\text{-}low} < \dot{Q}_{ctrl} \leq \dot{Q}_{HP\text{-}med} \\ \dot{Q}_{HP\text{-}med} & \text{if } \dot{Q}_{HP\text{-}med} < \dot{Q}_{ctrl} \leq \dot{Q}_{HP\text{-}high} \\ \dot{Q}_{HP\text{-}high} & \text{if } \dot{Q}_{ctrl} > \dot{Q}_{HP\text{-}high} \end{cases} \quad (7b)$$

2.4 Thermal Comfort

Acceptable upper and lower temperatures for residential buildings, as suggested by Peeters *et al.* (Peeters et al., 2009), are given by Equations (8a) and (8b), respectively, where T_n is the indoor temperature, w is the width of the comfort band in °C, and α is a constant ≤ 1. The study suggests that $w = 5$ and $\alpha = 0.7$ incur in 90% acceptability. T_n is computed as shown in Equation (8c), where T_{O-avrg} is the daily average of the ambient outdoor temperature. The total time (in hours) during which the indoor temperature is ourside the comfort band, t_{Disc}, can be computed as shown in Equation (9), where i indicates each simulation time step and J is the duration of the simulation time step in seconds. Variations in temperature also affect thermal comfort. Regarding cycling temperature, ASHRAE standard 55-2004 (ANSI/ASHRAE 55-2004, 2004) states that, if the peak variation exceeds 1.1 °C, the rate of temperature change shall not exceed 2.2 °C/h.

$$T_{upper} = T_n + w\alpha \quad (8a)$$

$$T_{lower} = T_n - w(1-\alpha) \quad (8b)$$

$$T_n = 20.4 + 0.06\, T_{O\text{-}avrg} \quad (8c)$$

$$Disc(i) = \begin{cases} 0 & \text{if } T_{lower} \leq T_H(i) \leq T_{upper} \\ 1 & \text{if } T_H(i) < T_{lower} \text{ or } T_H(i) > T_{upper} \end{cases} \quad (9a)$$

$$t_{Disc} = \frac{J}{3600} \sum_{i=1}^{24(3600/J)} Disc(i) \text{ (time in hours)} \quad (9b)$$

2.5 Power Usage and Cost Assessment

The electric power, P_{HP}, consumed by the heat pump at every simulation time step, i, is computed using Equation (10), relating heat transfer to electrical power consumption via the heat pump coefficient of performance (COP). The total cost, C_{total}, for operating the system for one day can be computed based on the time of use rates (TUR), as shown in Equation (11). Where J is the duration of the simulation time step in seconds. Electricity consumption by the FCS is not included in the cost analysis.

$$P_{HP}(i) = \frac{\dot{Q}_{HP}(i)}{COP(\dot{Q}_{HP}(i), T_O(i))} \quad (10)$$

$$C_{total} = \sum_{i=1}^{24(3600/J)} P_{HP}(i) TUR(i) T \quad (11)$$

3 SIMULATION SETTINGS

3.1 Model Parameters

We consider a 600 m^3 house (21188.8 cubic feet). The heat capacity of the house, $C_H m_H = 37968\ kJ.K^{-1}$, includes the heat capacity of its structure and volume of air. The heat capacity of the air contained in the house was calculated from its volume, density (1.2041 $kg.m^{-3}$), and specific heat (1.005 $kJ.kg^{-1}.K^{-1}$). The heat capacity of the house

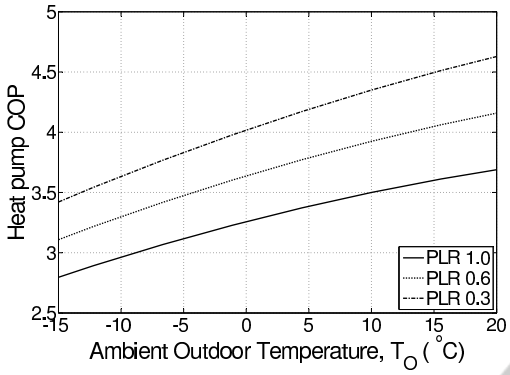

Figure 2: Heat pump coefficient of performance (COP) as a function of ambient outdoor temperature, T_O, and part-load ratio (PLR).

structure was calculated based on the method described in (Olsen and Rode, 2008); considering Gypsum plasterboard walls and ceilings 0.05 m thick, and concrete and tile flooring 0.1 m thick.

We consider a thermal storage unit of 150 gallons (approximately 568 L). The thermal capacitance of the thermal storage unit, $C_{TM}m_{TM} = 2376\ kJ.K^{-1}$, was calculated from its volume, the density of water (1.00 $kg.L^{-1}$), and the specific heat of water (4.185 $kJ.kg^{-1}.K^{-1}$). The thermal conductance of the storage insulation, $Y_L = 0.003\ kW.K^{-1}$, was calculated based on the typical electric water heater properties described in (DOE, 1998) (Table 8); considering a cylindrical storage of 35 inches in diameter.

The heat transfer coefficient related to the insulating properties of the house, $K_H = 0.2530\ kW.K^{-1}$, derives from the surface area and thermal resistivity of the home, and was calculated using the Oak Ridge National Laboratory Online Simple Whole Wall R-value Calculator (www.ornl.gov).

The heat transfer coefficients used for the FCS, $Y_{TM\text{-}H}$, was derive from Equation (2a), considering there is no heat exchange with the outside, i.e. $K_H = 0$; and the thermal mass is at a constant 65 °C. The values for $Y_{FC\text{-}high}$ and $Y_{FC\text{-}low}$ were chosen so as to increase the indoor temperature from 16 to 20 °C in 30 and 60 minutes respectively.

We consider a three-ton multistage heat pump, adopting a COP model from Jeter *et al.* (Jeter et al., 1987) that allows for COP to vary as a function of both ambient outside temperature and compressor speed. COP ranges represent a typical multi-speed heat pump. The three operation modes, $\dot{Q}_{HP\text{-}low}$, $\dot{Q}_{HP\text{-}med}$ and $\dot{Q}_{HP\text{-}high}$, correspond to 0.3, 0.6 and 1 part-load ratios (PLR) respectively. Figure 2 shows the COP curves for each PLR.

The target indoor temperature, $T_{H\text{-}goal}$, was 21 °C. This temperature is the approximate center of comfort range for the chosen weather profiles. The target thermal mass temperature, $T_{TM\text{-}goal}$, was 65 °C, which is high enough to kill harmful bacteria in the water, but not so high as to risk scalding in case of accident.

Model parameter values are summarized in Table 1.

Table 1: Model parameters.

parameter	value	unit
$C_{TM}m_{TM}$	2 376	kJ/K
C_Hm_H	37 968	kJ/K
K_H	0.2530	kW/K
$Y_{FC\text{-}high}$	1.800	kW/K
$Y_{FC\text{-}low}$	0.900	kW/K
Y_L	0.003	kW/K
$\dot{Q}_{HP\text{-}low}$	3.15	kW
$\dot{Q}_{HP\text{-}med}$	6.30	kW
$\dot{Q}_{HP\text{-}high}$	10.5	kW
$T_{H\text{-}goal}$	21	°C
$T_{TM\text{-}goal}$	65	°C
k_P	1	kW/K
k_D	5	kJ/K

Table 2: Time of use rates for winter months.

	time	rate [cents/kWh]
on-peak	06:00 to 10:00 17:00 to 20:00	13.266
mid-peak	10:00 to 17:00 20:00 to 22:00	7.500
off-peak	22:00 to 06:00	4.422

3.2 Simulation Parameters

The TUR reflect the winter rates in use by Portland General Electric, as shown in Table 2, and were applied equally to all three locations. Three weather profiles are considered: the average hourly temperatures for January 1st in Portland, OR; Halmstad, Sweden; and Colorado Springs, CO; as shown in Figure 3.

Temperature control cases I through IV are simulated for each of the three outdoor temperature profiles. The demand response program requires the heat pump to switch off during peak time-of-use rates (TUR). Total power usage and cost were calculated for each scenario. Initial values for T_H and T_{TM} were 21 and 65 °C respectively. The chosen simulation time step J is 60 seconds, and the total simulation time is 24 hours. Simulations are performed using Acumen (www.acumen-language.org) (Taha et al., 2011), a modeling language where models are defined through differential equations and simulations are generated automatically.

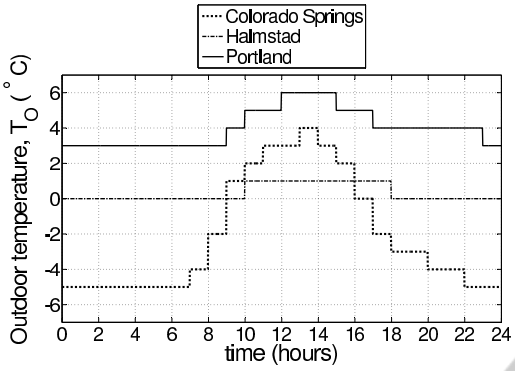

Figure 3: Weather profiles for Portland, Colorado Springs and Halmstad. Average hourly outdoor temperature for the month of January in each of the locations.

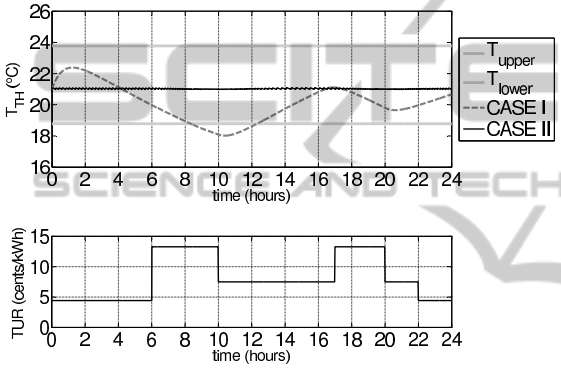

Figure 4: Indoor temperature, T_H, and time-of-use rates (TUR) for cases I and II, Colorado Springs weather profile.

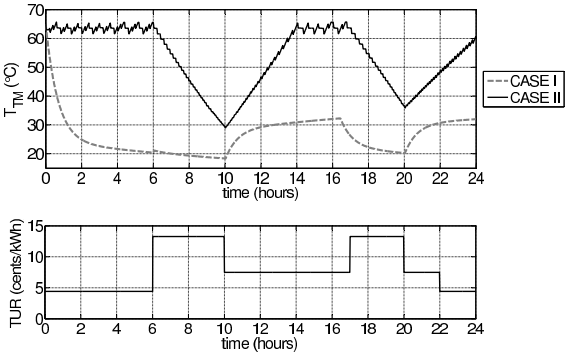

Figure 5: Thermal mass temperature, T_{TM}, and time-of-use rates (TUR) for cases I and II, Colorado Springs weather profile.

4 RESULTS

Control cases I and II represent a typical one-DoF system and the proposed two-DoF system respectively, both under similar on/off control strategies. The simulation results for indoor and thermal mass temperature, contrasting these two cases under the Colorado Springs weather profile, are shown in Figures 4 and 5 respectively. Very similar results were obtained for simulations under Halmstad and Portland weather profiles.

Table 3: Thermal comfort.

	Case I	Case II	Case III	Case IV
Colorado Springs				
t_{Disc} [hours]	4.02	0	0	0
mean T_H [°C]	20.11	21.02	21.02	21.01
cyclic ΔT_H [°C]	4.37	0.12	0.12	0.10
cyclic $\dot{T}_H$ [°C/h]	0.58	-	-	-
Halmstad				
t_{Disc} [hours]	1.45	0	0	0
mean T_H [°C]	20.44	21.03	21.02	21.02
cyclic ΔT_H [°C]	3.79	0.12	0.12	0.10
cyclic $\dot{T}_H$ [°C/h]	0.50	-	-	-
Portland				
t_{Disc} [hours]	0	0	0	0
mean T_H [°C]	20.66	21.04	21.03	21.03
cyclic ΔT_H [°C]	3.29	0.12	0.12	0.10
cyclic $\dot{T}_H$ [°C/h]	0.60	-	-	-

Results show that the response of the one-DoF system (Case I) varies greatly and slowly. The indoor temperature starts considerably high because the initial thermal mass temperature is 65°C. The thermal mass temperature must decrease considerably in order to maintain the indoor temperature within the comfortable range. Another drawback of the one-DoF system is that during peak-hours, when the heat pump is off, the temperature of the house falls considerably below the limits of thermal comfort Figure 4. The additional DoF introduced by the FCS (Case II) allows the thermal mass temperature to vary considerably from 65 down to approximately 30 °C, Figure 5, while the indoor temperature strays very little from the goal temperature of 21 °C, Figure 4.

A summary of the indoor temperature results for each of the simulated scenarios is shown in Table 3. Note that the traditional one-DoF system simulated in Case I results in indoor temperatures outside the comfortable limits for both Colorado Springs and Halmstad weather profiles. The two-DoF system simulated in Cases II through IV, on the other hand, maintain the indoor temperature very close to 21°C with less than 0.2 °C of peak-to-peak cyclic variations.

Figure 6 shows the heat pump output, Q_{HP}, and thermal mass temperature, T_{TM}, for cases II through IV for the Colorado Springs weather profile. In all cases, the thermal mass temperature profile is very similar. Case II shows slightly larger cyclic oscillations due to the on/off duty cycles. The same patterns were observed for simulations under Halmstad and Portland weather profiles.

A summary of the thermal mass temperature be-

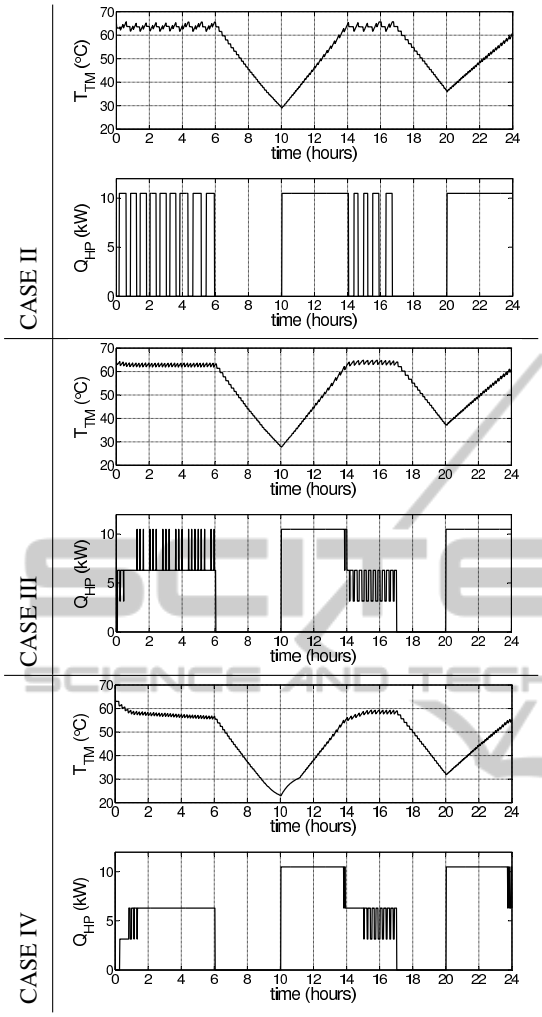

Figure 6: Thermal mass temperature, T_{TM}, and heat pump output, Q_{HP}, for cases II though IV, Colorado Springs weather profile.

Table 4: Thermal storage.

	Case I	Case II	Case III	Case IV
Colorado Springs				
max T_{TM} [°C]	65.00	65.69	65.00	65.00
min T_{TM} [°C]	18.37	28.99	27.76	22.95
mean T_{TM} [°C]	26.15	53.32	53.07	47.48
Halmstad				
max T_{TM} [°C]	65.00	65.78	65.00	65.00
min T_{TM} [°C]	19.13	31.08	32.14	26.90
mean T_{TM} [°C]	26.02	55.36	55.53	50.19
Portland				
max T_{TM} [°C]	65.00	65.78	65.14	65.00
min T_{TM} [°C]	19.65	36.93	37.70	31.98
mean T_{TM} [°C]	25.34	57.91	58.35	53.04

havior for all control cases is shown in Table 4. Note that the mean temperatures for Case I are considerably below the intended temperature of 65 °C.

Table 5: Power consumption and cost.

	Case I	Case II	Case III	Case IV
Colorado Springs				
Power [kWh]	33.447	41.940	42.806	40.935
Cost [USD]	2.31	2.56	2.63	2.56
Halmstad				
Power [kWh]	30.312	37.726	42.806	35.858
Cost [USD]	2.07	2.40	2.63	2.31
Portland				
Power [kWh]	23.543	29.505	30.364	28.502
Cost [USD]	1.57	1.90	1.94	1.85

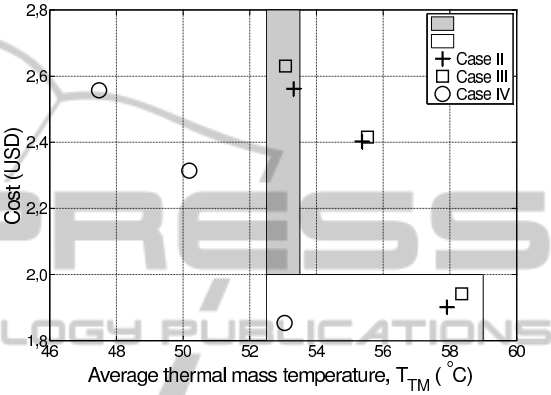

Figure 7: Average thermal mass temperature versus cost for control cases II, III, and IV. The gray box highlights that cases I and II incur a cost of approximately 2,6 USD to maintain a mean temperature of about 53 °C, whereas case IV maintains the same mean temperature for only 1,85 USD. The clear box highlights that control cases II and III are able to achieve an average temperature approximately 5 °C higher than case IV for an increased cost of less than 0,10 USD.

The power usages and costs for each simulated scenarios are shown in Table 5. Case I consumes considerably less energy than the other cases, however, it does not fulfill the thermal comfort requirements. Figure 7 shows a plot of mean thermal mass temperature against cost for control cases II through IV under all three weather profiles. The gray box in Figure 7 highlights that cases I and II incur a cost of approximately 2,6 USD to maintain a mean temperature of about 53 °C, whereas case IV maintains the same mean temperature for only 1,85 USD. Note also that control cases II and III are able to achieve an average temperature approximately 5 °C higher than case IV for an increased cost of less than 0,10 USD, highlighted by the clear box in Figure 7.

5 DISCUSSION

The proposed two-degree-of-freedom system provides more flexibility for DR programs. By decoupling the heat pump output from the indoor temperature, the thermal storage can be used to store more energy, as evidenced by the higher thermal mass temperatures for Cases II through IV. The direct coupling of the heat pump output and the indoor temperature in Case I suggests that there is need for more advanced predictive control strategies, specifically ones that can pre-heat the structure in anticipation of peak time-of-use rates or extreme weather. Such predictive control, however, would not be able to cope with accidental power loss or other unforeseeable issues. Having a thermal storage, able to operate at higher temperatures, makes the system more robust and more flexible.

Simulation results show that a heat pump operates at maximum output when switching on immediately after peak pricing hours end. This occurs because the heat pump must compensate for the large thermal energy loss incurred during peak pricing hours. This reconnection effect may increase power consumption overall, and shift the peak periods instead of lessening them. The effects of reconnecting appliances after a forced disconnection has been studied, e.g. (Ericson, 2009), and control strategies have been designed to minimize this reconnection effect for water heaters, e.g. (Nehrir et al., 1999). In the case of space heating, the reconnection spike may be reduced by making the controller aware of current and predicted weather, or pre-heating in anticipation of peak TUR. Reconnection costs and mitigating strategies will be investigated in future works.

It is important to note that the control strategies proposed here were not optimized in any way. Lower goal temperatures for the thermal mass, for example, are likely to result in lower power consumption. However, we implemented very simple and intuitive controllers for the purpose of comparing different control strategies that resulted in similar thermal mass and house temperature profiles. There are many research opportunities for optimization schemes that take into account real-time pricing, weather predictions, and other factors.

This paper investigates the behavior of single isolated systems, where the only outside inputs were weather and time-of-use rates. This facilitated an understanding of system properties. The next step is to understand the impact of thousands of such systems being used for DR. Monte Carlo methods can be used to simulate a large number of these systems with slightly different parameters so as to model the slight differences between real houses. However, in order to develop a practical system model, parameters must be validated against practical experiments. Future works will focus on more realistic and large scale simulations.

Customer willingness to participate in DR programs increases as the benefits they derive exceed the cost of the inconvenience (Fahrioğlu and Alvarado, 2000). Minimizing or eliminating discomforts should lead to increased participation in such programs. Despite the simplifications made in this study, our results show that an insulted thermal storage unit coupled to a heat pump and forced convection system for space heating may be used in price-based demand response programs without either compromising the thermal comfort of the residents nor requiring they modify their behavior by deferring consumption to a later time period. This proposed system, therefore, could be a means by which to increase participation levels within utility DR programs.

6 CONCLUSION

Demand response programs are effective and relatively inexpensive ways to cope with peak demands; balance demand and generation; and stabilize electricity prices. Water heaters and HVAC systems are commonly used for DR. This paper introduces a space heating system composed of an insulated thermal mass and forced convection system with two degrees of control freedom that can be used for DR. The thermodynamic model was presented as well as four different temperature control strategies. Simulations were used to evaluate the performance of the system based on thermal comfort and power consumption in three different weather regions. Results show that the FCS introduces an important degree of freedom that improves indoor temperature control while at the same time allowing the temperature of the thermal mass to vary more freely. The power consumption of the system can vary greatly according to the control strategy and the insulating properties of the house. Future research avenues include investigating optimized control strategies that account for real-time pricing, weather forecasts, occupancy patterns, among others; and, investigating the aggregate demand response of large numbers of homes equipped with heat pumps, forced convection and controllable thermal masses.

ACKNOWLEDGEMENTS

Partial funding for this research was provided by Portland General Electric (PGE). PGE played no role in the design and analysis of the study, nor the interpretation of findings. Nor did PGE participate in the writing of this report or the decision to submit this article for publication.

REFERENCES

Albadi, M. and El-Saadany, E. (2007). Demand response in electricity markets: An overview. In *Power Engineering Society General Meeting, 2007. IEEE*, pages 1 –5.

ANSI/ASHRAE 55-2004 (2004). Thermal environmental conditions for human occupancy. ASHRAE 55-2004. ANSI Approved.

Chassin, D., Hammerstrom, D., and DeSteese, J. (2008). The pacific northwest demand response market demonstration. In *Power and Energy Society General Meeting - Conversion and Delivery of Electrical Energy in the 21st Century*, pages 1–6.

Diao, R., Lu, S., Elizondo, M., Mayhorn, E., Zhang, Y., and Samaan, N. (2012). Electric water heater modeling and control strategies for demand response. In *Power and Energy Society General Meeting, 2012 IEEE*, pages 1 –8.

DOE (1998). Results and methodology of the engineering analysis for residential water heater efficiency standards. US Department of Energy, Office of Codes and Standards.

Du, P. and Lu, N. (2011). Appliance commitment for household load scheduling. *Smart Grid, IEEE Transactions on*, 2(2):411–419.

Ericson, T. (2009). Direct load control of residential water heaters. *Energy Policy*, 37(9):3502 – 3512.

Fahrioğlu, M. and Alvarado, F. (2000). Designing incentive compatible contracts for effective demand management. *Power Systems, IEEE Transactions on*, 15(4):1255 –1260.

Fuller, J., Schneider, K., and Chassin, D. (2011). Analysis of residential demand response and double-auction markets. In *Power and Energy Society General Meeting, 2011 IEEE*, pages 1–7.

Jeter, S., Wepfer, W., Fadel, G., Cowden, N., and Dymek, A. (1987). Variable speed drive heat pump performance. *Energy*, 12(12):1289 – 1298.

Kondoh, J., Lu, N., and Hammerstrom, D. (2011). An evaluation of the water heater load potential for providing regulation service. *Power Systems, IEEE Transactions on*, 26(3):1309 –1316.

Lu, N. (2012). An evaluation of the hvac load potential for providing load balancing service. *Smart Grid, IEEE Transactions on*, 3(3):1263–1270.

Lu, N., Chassin, D., and Widergren, S. (2005). Modeling uncertainties in aggregated thermostatically controlled loads using a state queueing model. *Power Systems, IEEE Transactions on*, 20(2):725–733.

Mohsenian-Rad, A.-H., Wong, V., Jatskevich, J., Schober, R., and Leon-Garcia, A. (2010). Autonomous demand-side management based on game-theoretic energy consumption scheduling for the future smart grid. *Smart Grid, IEEE Transactions on*, 1(3):320–331.

Molina-Garcia, A., Kessler, M., Fuentes, J., and Gomez-Lazaro, E. (2011). Probabilistic characterization of thermostatically controlled loads to model the impact of demand response programs. *Power Systems, IEEE Transactions on*, 26(1):241–251.

Nehrir, M., LaMeres, B., and Gerez, V. (1999). A customer-interactive electric water heater demand-side management strategy using fuzzy logic. In *Power Engineering Society 1999 Winter Meeting, IEEE*, volume 1, pages 433 –436 vol.1.

Olsen, L. and Rode, C. (2008). Heat capacity in relation to the danish building regulation. In *Proceedings of the 8th Symposium on Building Physics in the Nordic Countries: Selected papers*, volume 3, pages 16–18.

Peeters, L., de Dear, R., Hensen, J., and D'haeseleer, W. (2009). Thermal comfort in residential buildings: Comfort values and scales for building energy simulation. *Applied Energy*, 86(5):772 – 780.

Pipattanasomporn, M., Kuzlu, M., and Rahman, S. (2012). An algorithm for intelligent home energy management and demand response analysis. *Smart Grid, IEEE Transactions on*, 3(4):2166–2173.

RECS (2001). Residential energy consumption surveys. US Energy Information Administration, Office of Energy Markets and End Use.

Saele, H. and Grande, O. (2011). Demand response from household customers: Experiences from a pilot study in norway. *Smart Grid, IEEE Transactions on*, 2(1):102 –109.

Schneider, K., Fuller, J., and Chassin, D. (2011). Analysis of distribution level residential demand response. In *Power Systems Conference and Exposition (PSCE), 2011 IEEE/PES*, pages 1–6.

Shao, S., Pipattanasomporn, M., and Rahman, S. (2013). Development of physical-based demand response-enabled residential load models. *Power Systems, IEEE Transactions on*, 28(2):607–614.

Spees, K. and Lave, L. B. (2007). Demand response and electricity market efficiency. *The Electricity Journal*, 20(3):69 – 85.

Taha, W., Brauner, P., Cartwright, R., Gaspes, V., Ames, A., and Chapoutot, A. (2011). A core language for executable models of cyber physical systems: work in progress report. *SIGBED Rev.*, 8(2):39–43.